JOURNAL OF Materials CHEMISTRY

Matrix dependence of light emission from TCNQ adducts

David Bloor,*[a] Yasuyuki Kagawa,[a]† Marek Szablewski,[a] Mosurkal Ravi,[a] Stuart J. Clark,[a] Graham H. Cross,[a] Lars-Olof Pålsson,[a] Andrew Beeby,[b] Chetin Parmer[c] and Garry Rumbles[c]‡

[a]*Department of Physics, University of Durham, South Road, Durham, UK DH1 3LE*
[b]*Department of Chemistry, University of Durham, South Road, Durham, UK DH1 3LE*
[c]*Department of Chemistry, Imperial College London, Exhibition Road, London, UK SW7 2AY*

Received 5th June 2001, Accepted 18th September 2001
First published as an Advance Article on the web 31st October 2001

The reactions of primary and secondary amines with 7,7,8,8-tetracyano-*p*-quinodimethane§ (TCNQ) lead to mono- and di-substituted adducts. Fluorescence emission has been observed for several of these compounds. The luminescence property of the TCNQ adducts, 2-{4-[(2,6-dimethylmorpholin-4-yl)(4-methylpiperidin-1-yl)methylene]cyclohexa-2,5-dien-1-ylidene}malononitrile (MORPIP) and 2-{4-[cyclohex-1-yltetrahydropyrimidin-2(1*H*)-ylidene]cyclohexa-2,5-dien-1-ylidene}malononitrile (AMINO) were investigated in a variety of environments. These included alcohol solutions and crystals at room temperature and glass forming solvents and polymer films as a function of temperature. The fluorescence quantum yields and Stokes' shifts were found to be very sensitive to the matrix. Crystal structure data show that the molecules are non-planar in the ground state. The matrix effect is discussed in terms of the conformational change during photo-excitation and the constraint imposed on this by the matrix.

1. Introduction

Since the first synthesis[1] and study of the basic chemistry[2] of TCNQ in 1962, the chemistry of adducts of TCNQ has been extensively explored.[3–5] Recently this class of compounds has attracted interest because of their non-linear optical properties. While much of this work has focussed on single crystals and the large molecular hyperpolarisibity (β) of these compounds[6–9] they have also been shown, both experimentally and theoretically, to possess large ground state dipole moments (μ).[10,11] The product $\mu\beta$, which is large in these materials, is a useful molecular figure of merit characterising the second order non-linearity of poled polymer films containing the chromophores.[12] Thus, there is continuing interest in these TCNQ adducts as components of electro-optical polymers. In contrast, the fluorescence of non-linear optical chromophores has attracted little attention. Generally it has been regarded as a problem since fluorescence excited by either harmonics or two-photon absorption can affect measurements of non-linear optical coefficients, even when the fluorescence from the chromophores is weak. However, we have discovered that certain of our TCNQ adducts show intense, matrix dependent fluorescence.[11,13]

Interest in organic light emitting chromophores has expanded rapidly since the discovery of efficient electro-luminescence (EL), its use in light emitting devices[14–16] and its potential for electrically pumped solid state lasers.[17,18] The measurement of photo-luminescence has been used extensively to characterise fluorescent chromophores and identify potential materials for use in EL devices. Measurements of radiative lifetimes and fluorescence quantum yields of fluorophores are routinely performed in solution.[19] Fluorescence in solution is affected by solvent polarity, the solvatochromism observed for polar molecules can be very large.[20] Fluorescence is also affected by solvent viscosity.[21] Alcohols provide a solvent system where both polarity and viscosity can be varied. The polarity of the solvent can be changed for normal alcohols by extending the molecular length.[22,23] The viscosity of the solvent can be controlled by changing the number of hydroxy groups, this leads to the enhancement of the hydrogen bonding network in the medium and increased viscosity, *e.g.* as in diethylene glycol and glycerol.[24,25] A study of fluorescence lifetimes and quantum yields was undertaken for two of our chromophores, 2-{4-[(2,6-dimethylmorpholin-4-yl)(4-methylpiperidin-1-yl)methylene]cyclohexa-2,5-dien-1-ylidene}malononitrile (MORPIP) and 2-{4-[cyclohex-1-yltetrahydropyrimidin-2(1*H*)-ylidene]cyclohexa-2,5-dien-1-ylidene}malononitrile (AMINO), dissolved in a series of normal alcohols, diethylene glycol and glycerol to evaluate the influence of the viscosity and polarity of the medium on their luminescence properties.

The fluorescence was first observed visually from a MORPIP sample placed adjacent to an ultra-violet lamp used for exciting fluorescence on TLC plates. A bright yellow emission was observed from crystalline material deposited inside a test tube above a weakly fluorescing acetonitrile solution. This observation indicated that the environment of the chromophore had a large effect on the emission. Studies were therefore undertaken of crystalline powders and molecules dispersed in solid, amorphous matrices. These included glass-forming solvents at low temperature and polymers. The latter were studied as the incorporation of fluorophores into polymer matrices has been used in the fabrication of electro-luminescent devices. The quantum efficiency of the fluorescence was found to depend on both matrix and temperature. Details of the study of the fluorescence of these TCNQ adducts in solution and solid matrices are presented here and complement our earlier brief communication.[13]

†Present address: Corning International, Communications Products Div., No.35 Kowa Bld. 3rd Flr., 14-14 Akasaka-chome, Minato-chu, Tokyo 107-0052, Japan.
‡Present address: National Renewable Energy Laboratory, MS3216, 1617 Cole Blvd, Golden, CO 80401, USA.
§The IUPAC name for TCNQ is (cyclohexa-2,5-diene-1,4-diylidene)-dimalononitrile.

DOI: 10.1039/b104992p

2. Experimental

TCNQ of 98% purity was obtained from Lancaster Ltd. 2,6-Dimethylmorpholine, 4-methylpiperidine and *N*-(3-aminopropyl)cyclohexylamine of 97% purity were obtained from Aldrich Ltd. All solvents used were HPLC grade. These chemicals were used without further purification.

2.1 Synthesis

2.1.1 2-{4-[(2,6-Dimethylmorpholin-4-yl)(4-methylpiperidin-1-yl)methylene]cyclohexa-2,5-dien-1-ylidene}malononitrile (MORPIP). 2-{4-[(2,6-Dimethylmorpholin-4-yl)(4-methylpiperidin-1-yl)methylene]cyclohexa-2,5-dien-1-ylidene}malononitrile (MORPIP) was prepared in a two-stage reaction. 2,6-Dimethylmorpholine (0.527 ml, 4.8 mmol) was added to a solution of TCNQ (1 g, 4.8 mmol) in 100 ml tetrahydrofuran (THF) heated at 50 °C. The mixture was stirred at 50 °C for 3 hours, cooled to room temperature and then stirred overnight. The solvent was removed under vacuum. The residue was re-crystallised in acetonitrile twice and dried under vacuum. 0.52 g of 2-{4-[1-(2,6-dimethylmorpholin-4-yl)-2-nitriloethylidene]-cyclohexa-2,5-dien-1-ylidene}malononitrile, yield 36%, was obtained. 4-Methylpiperidine (0.2 ml, 2 mmol) was added to a solution of 2-{4-[1-(2,6-dimethylmorpholin-4-yl)-2-nitrilo-ethylidene]cyclohexa-2,5-dien-1-ylidene}malononitrile (0.4 g, 1.36 mmol) in THF (30 ml) heated at 50 °C and stirred for 30 min at 50 °C. The product was observed to precipitate. The solution was cooled to room temperature and stirred for one hour. The yellow precipitate was collected by filtration and dried under vacuum. Re-crystallisation of the solid was carried out with acetonitrile. Yellow crystals of MORPIP were obtained (0.24 g, 46%). Analytical data: λ_{max} 417 nm in acetonitrile. Microanalysis, calculated for $C_{22}H_{28}N_4O$: % C 72.5, H 7.74, N 15.37, found: % C 72.13, H 7.70, N 15.18. Mass spectrum (EI): 364(M^+) (100%, molecular ion). Decomposition temperature 260 °C. The molecular structure was confirmed by X-ray crystallography,[5] detailed accounts of X-ray crystallographic data for TCNQ adducts will be presented elsewhere.[26]

2.1.2 2-{4-[Cyclohex-1-yltetrahydropyrimidin-2(1*H*)-ylidene]cyclohexa-2,5-dien-1-ylidene}malononitrile (AMINO). 2-{4-[Cyclohex-1-yltetrahydropyrimidin-2(1*H*)-ylidene]cyclohexa-2,5-dien-1-ylidene}malononitrile (AMINO) was prepared by adding *N*-(3-aminopropyl)cyclohexylamine (0.5 ml, 2.8 mmol) to TCNQ (0.5 g, 2.4 mmol) in acetonitrile (30 ml) heated to 50 °C. The mixture was stirred at 50 °C for three hours and cooled to room temperature. The product precipitated and was collected by filtration. The precipitate was recrystallised from acetone and dried under vacuum. A brown powder (0.23 g, yield 31.1%) was obtained. Analytical data: ^{1}H NMR: (*d*-DMSO), δ 7.1 ppm, doublet, benzene protons (2H); δ 6.8 ppm, doublet, benzene protons (2H); δ 3.6 ppm, quintet, amine proton (1H); δ 3.45 ppm, triplet; -(CH_2)- next to NH (2H); δ 3.35 ppm, triplet, -(CH_2)- next to N (2H); δ 1.95 ppm, triplet; cyclohexane proton next to N (1H); δ 1.7 and 1.0 ppm, cyclohexane and -(CH_2)- protons (12 H). IR: 2179, 2132 cm^{-1} (nitrile stretching). λ_{max}: 368 nm in acetonitrile. Microanalysis: Calcd for $C_{19}H_{22}N_4$: % C 74.48, H 7.24, N 18.28. Found: % C 74.46, H 7.35, N 18.28. Mass spectrum (EI): 306(M^+) (100%, molecular ion). Decomposition temperature: 220 °C.

The NMR spectrum was recorded in *d*-DMSO, a polar solvent. Therefore, the aromatic protons sense different electronic environments due to the charge separation between the donor and acceptors groups. These protons are observed as doublets at δ 7.1 and 6.8 ppm. This splitting is observed in other TCNQ adducts.[10]

2.2. Physical characterisation

Room temperature emission and photo-excitation spectra were recorded with a Perkin–Elmer Luminescence Spectrometer, LS-50B, and absorption spectra were recorded with a Perkin–Elmer Lambda 19 spectrophotometer. MORPIP solutions were prepared in methanol, ethanol, propan-1-ol, butan-1-ol, pentan-1-ol, hexan-1-ol, ethylene glycol, and glycerol without degassing. After filtration (0.5 μm filters) solutions were diluted to give an optical density 0.055 ± 0.01 at 375 nm. A reference solution of quinine sulfate dihydrate in 0.5 M sulfuric acid with the same optical density was also prepared. The quantum yield of quinine sulfate dihydrate is 0.55 and is relatively temperature independent.[27] The quantum yields of the MORPIP solutions were calculated by comparing the integrated emission intensity of the quinine sulfate dihydrate solution to that of samples. All of the emission spectra were measured with the same spectral resolution.

Thin films of poly(methylmethacrylate) (PMMA) and bisphenol A poly(carbonate) (PC) were prepared as described in the following example. MORPIP (11 mg) and PMMA pellets (1.218 g) were dissolved in 3 ml of tetramethylurea (TMU). The mixture was stirred for several days to ensure complete dissolution. Glass substrates were cleaned with acetone and a mixture of acetone and isopropyl alcohol. For films prepared by spin coating the PMMA solution was dropped on to the substrate and the spin coater was switched on. A spin rate of 2000 rpm for ten to fifteen seconds gave optically translucent PMMA films with thickness in the range 3–5 μm. Dip coated films were prepared by the slow withdrawal of the clean substrate from the solution giving films with thickness >10 μm. The films were kept in an oven at 80 °C for three to five days under vacuum to ensure complete removal of solvent prior to spectral measurements.

The photoluminescence quantum yield (PLQY) of polymer thin films prepared as described above, and polycrystalline samples deposited on to Spectrosil substrates was determined at room temperature using an integrating sphere (Labsphere) to collect the light emitted in all directions.[28] The excitation was provided by the 442 nm line of a CW HeCd laser (Kimmon) and the excitation intensity was about 0.5 mW on an area of 2 mm^2. Absorbance of the samples at the excitation wavelength was in the range 0.3 to 0.5.

Low temperature emission and photo-excitation spectra were recorded with an ISA Fluoromax fluorimeter. Low temperature absorption spectra were recorded with a Perkin–Elmer Lambda 15 spectrophotometer. MORPIP solutions were prepared in glass forming solvents, either propan-1-ol, 2-methyltetrahydrofuran (2MTHF) or EPA, a 2 : 2 : 5 mixture of ether, ethanol and isopentane. Typically the optical density of these solutions at the absorption maximum was below 0.5. The samples were placed in a special low temperature cuvette in an Oxford Instruments cryostat (DN1704). Absorption, emission and photo-excitation spectra were obtained in the range from room temperature to 80 K as the sample was varied with an Oxford Instrument temperature controller (ITC-6). Data were obtained for polymer thin film samples mounted in the same cryostat.

Fluorescence lifetimes were measured using the time-correlated single photon counting technique.[29] Samples were excited with a cavity dumped DCM dye laser (Coherent 7210 cavity dumper and 700 Series dye laser) that was synchronously pumped with the second harmonic of a mode locked Nd : YAG laser (Coherent Antares 76-s). The resulting 3.8 MHz pulse train could be tuned over the range 610–680nm. Excitation pulses in the range 300–340 nm of intensity approximately 10 pJ were obtained from this pulse train by frequency doubling in a BBO crystal. The detection system comprised a 0.22 m subtractive dispersion double monochromator (Spex 1680), a microchannel plate (Hamamatsu R3809U), a 1GHz amplifier

and timing discriminator (EG&G Ortec 9327), a time-to-amplitude converter (Tennelec TC864) and a multichannel pulse to height analyser (Tennelec PCA II). The inherent response time of the system was *ca.* 80 ps. Excitation and detection wavelengths were selected from the steady state data. Solutions in glass forming solvents and polymer films were prepared and mounted in the cryostat as described above. Fluorescence lifetimes were recorded at room temperature, 200 K, 125 K and 80 K.

3. Results

Fluorescence emission has been observed from many of the TCNQ adducts we have synthesised. The emission is more intense for the asymmetrically substituted adducts than for the symmetrically substituted compounds we have studied. We have, therefore, concentrated our studies on two asymmetrically substituted adducts one with two distinct substituents (MORPIP) and one with an asymmetrically substituted fused ring (AMINO). The structure of these compounds is, in general, intermediate between the two limiting forms, the neutral state with quinoid structure and the fully charge separated zwitterionic state with benzenoid structure,[5,10,26,30] which are shown in Fig. 1. The actual structure will be determined by the reaction field acting on the molecule,[10,31] which will depend on the environment, *e.g.* on solvent polarity. X-Ray crystallographic data show that the electron donor moieties (amino groups) and the π-conjugation unit (the benzene ring) are not coplanar.[6,9,26,30] The twist angle between the plane of the conjugation unit and the plane containing the two amino nitrogen atoms and the carbon atom they are bonded to is approximately 45°. In addition the observed and calculated ground state dipole moments are large.[6,10,11,13,32] Thus, these molecules are expected to show sizeable solvatochromism and be affected by the constraints placed on changes in molecular conformation by rigid matrices. Experimental data are presented below for the different media used as hosts for the chromophores.

The combined effect of the solvatochromic shift of the ground and excited electronic energy levels gives rise to a solvent dependent Stokes' shift. There is an extensive literature on the modelling of solvent–solute interactions.[33] However, a simple approach leading to the Lippert equation, is often adequate.[19,34–39] In terms of the relative permittivity (ε) and refractive index (n) of the medium the absorption and emission energies, relative to the gas phase values, are given by

$$\nu_{\max}^{\mathrm{abs}} = \nu_0^{abs} - \frac{2\mu_g(\mu_e-\mu_g)}{hca^3}\left[\left(\frac{\varepsilon-1}{2\varepsilon+1}\right)-\left(\frac{n^2-1}{2n^2+1}\right)\right] - \frac{2(\mu_e^2-\mu_g^2)}{hca^3}\left(\frac{n^2-1}{2n^2+1}\right) - C(\alpha,D) \quad (1)$$

$$\nu_{\max}^{\mathrm{em}} = \nu_0^{em} - \frac{2\mu_e(\mu_e-\mu_g)}{hca^3}\left[\left(\frac{\varepsilon-1}{2\varepsilon+1}\right)-\left(\frac{n^2-1}{2n^2+1}\right)\right] - \frac{2(\mu_e^2-\mu_g^2)}{hca^3}\left(\frac{n^2-1}{2n^2+1}\right) - C(\alpha,D) \quad (2)$$

where μ_e and μ_g are the excited and ground state dipole moments, a is the radius of the spherical Onsager cavity surrounding the solute molecule and $C(\alpha,D)$ describes the effects of molecular polarisibility and dispersion, which are usually treated as small and constant for polar molecules. The Stokes' shift is then given by the difference

$$\Delta\nu = \nu_{\max}^{\mathrm{abs}} - \nu_{\max}^{\mathrm{ems}} = \frac{2(\mu_e-\mu_g)^2}{hca^3}\left(\frac{\varepsilon-1}{2\varepsilon+1}-\frac{n^2-1}{2n^2+1}\right)+\mathrm{constant} \quad (3)$$

where $(((\varepsilon-1)/(2\varepsilon+1))-((n^2-1)/(2n^2+1))$ is the polarity or solvent density parameter (Δf). Different approaches lead to similar expressions for $\Delta\nu$ but with different polarity parameters.[34,40] All are modified if the effect of solvent molecule reorientation is included.[34,41] These expressions have all been used to describe the behaviour of chromophores in polar solvents with some degree of success. This reflects the inaccuracies in the models and similarity of the polarity parameters.[40] We chose to use the Lippert formalism to provide a consistent analysis of the experimental data. Deviations from the Lippert equation can result from specific solvent interactions,[19,42] and relaxation of the approximations involved in its derivation.[43,44]

The analysis of the solvent induced shift in absorption and emission maxima is usually based on eqns. (1) and (2) with a number of simplifying assumptions.[35,36,38,40] For example if the difference in the nature of the ground and excited states is small eqns. (1) and (2) can be written as:

$$\nu_{\max}^{\mathrm{abs}} = \nu_0^{abs} - \frac{2\mu_g(\mu_e-\mu_g)}{hca^3}\left[\left(\frac{\varepsilon-1}{2\varepsilon+1}\right)-\frac{1}{2}\left(\frac{n^2-1}{2n^2+1}\right)\right] \quad (4)$$

and

$$\nu_{\max}^{\mathrm{em}} = \nu_0^{em} - \frac{2\mu_e(\mu_e-\mu_g)}{hca^3}\left[\left(\frac{\varepsilon-1}{2\varepsilon+1}\right)-\frac{1}{2}\left(\frac{n^2-1}{2n^2+1}\right)\right] \quad (5)$$

The case of $\mu_e \gg \mu_g$ has also been considered.[35] However, as noted above the choice of polarity parameter is not crucial.[40]

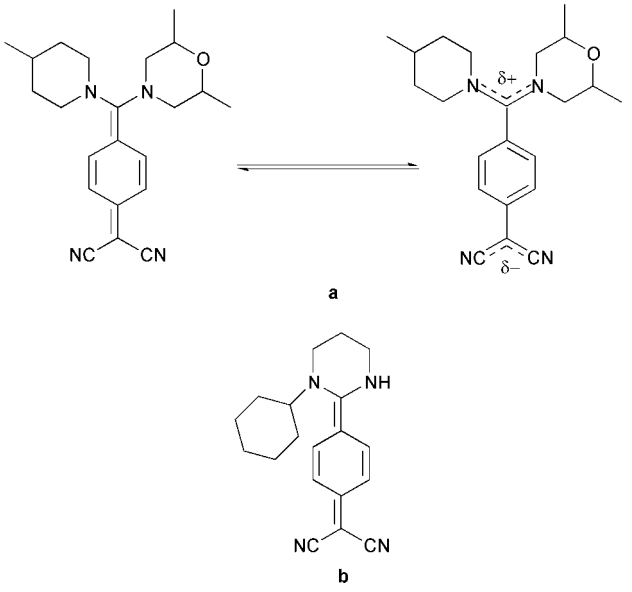

Fig. 1 Molecular structures of (*a*) MORPIP, shown in the extreme quinoid and benzenoid forms, and (*b*) AMINO, shown in the quinoid form.

3.1 Absorption and emission of alcohol solutions

The intensity of the room temperature emission from alcoholic solutions of MORPIP and AMINO show a strong solvent dependence. This is illustrated in Fig. 2, which shows the raw data for the emission of MORPIP solutions. Both emission and absorption spectra for MORPIP and AMINO are broad and featureless, scaled emission spectra and examples of absorption spectra are shown in Fig. 3. Comparison of absorption and fluorescence excitation spectra shows that they are identical within experimental error. The variation in the energy of the absorption maximum for MORPIP and AMINO dissolved in normal alcohols, methanol to hexanol, are plotted using eqn. (4) in Fig. 4. Similar results are obtained for a wider range of solvents, *i.e.* THF, dichloromethane, acetone, dimethylformamide (DMF) and acetonitrile. This trend is not maintained

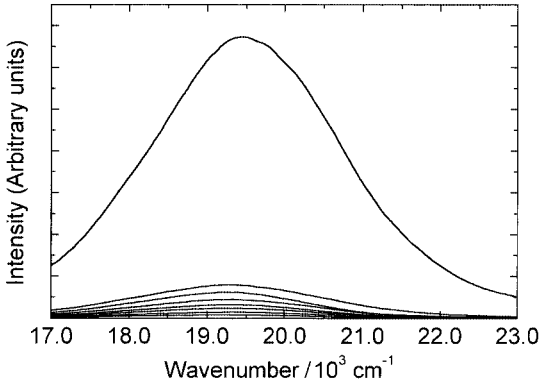

Fig. 2 Unscaled emission spectra of MORPIP in alcoholic solvents. From least to most intense spectra the solvents are methanol, ethanol, propanol, butanol, pentanol, hexanol, diethylene glycol and glycerol.

for chloroform, a somewhat less polar solvent. The hypsochromic shift for the more polar solvents is a result of the stabilisation of the benzenoid "zwitterionic" structure so that $\mu_e < \mu_g$. In low polarity solvents the molecules will be close to the intermediate, equal bond length structure.

Although all the emission profiles are similar the Stokes' shift and quantum yields for MORPIP and AMINO vary considerably, as shown in Table 1. The use of degassed solvent gave a slightly higher value for the quantum yield, however, the difference was within the error quoted in Table 1. The dependence of the Stokes' shifts on Δf for the normal alcohol solutions is plotted in Fig. 4 together with the absorption data.

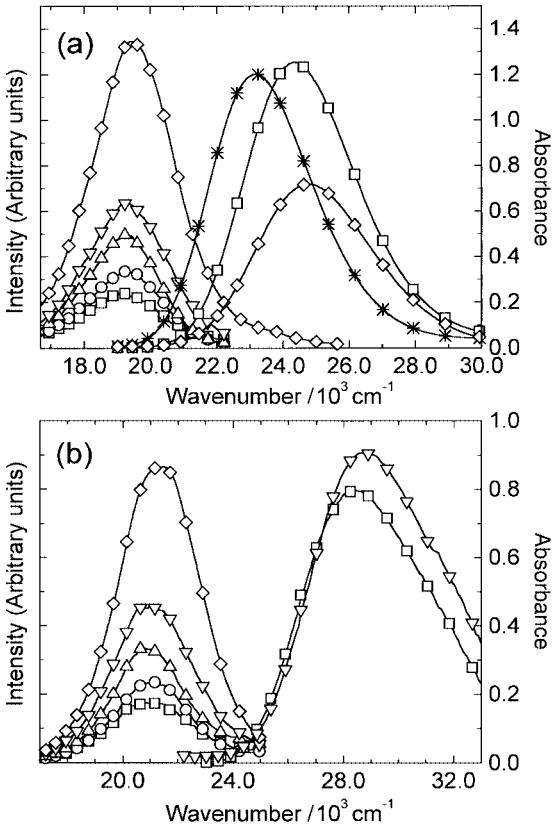

Fig. 3 Absorption (to the right) and emission spectra (to the left) for (a) MORPIP and (b) AMINO in solution in methanol (squares), propanol (circles), hexanol (triangles), pentanol (star), diethylene glycol (inverted triangles), and glycerol (diamonds). The fluorescence spectra have been multiplied in (a) by factors of 15, 7, 4, 4 and 1 and in (b) by factors of 20, 10, 6, 5 and 1 for methanol, propanol, hexanol, diethylene glycol and glycerol solutions respectively. The emission was excited at the peak of the photo-excitation spectrum at 375 nm.

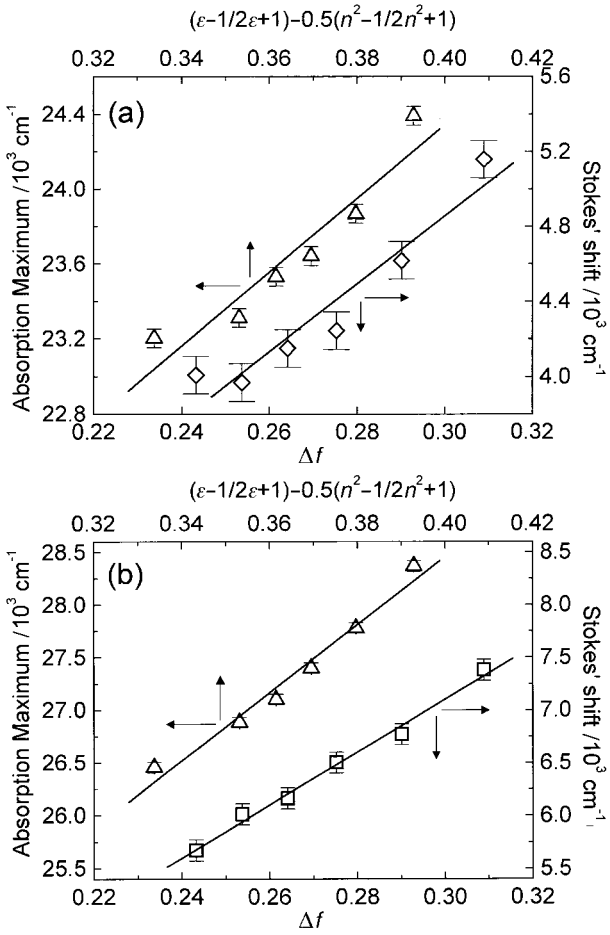

Fig. 4 The energy of the absorption maximum (triangles) and Stokes' shift (diamonds) plotted according to eqns. (3) and (4) for (a) MORPIP and (b) AMINO dissolved in normal alcohols (methanol to hexanol).

For MORPIP the slopes of the best-fit lines to both sets of data are the same within the fitting error, while for AMINO the slopes are similar. These results indicate that for these solutions the change in dipole moment between the excited and the ground states must be approximately constant and, from eqns. (4) and (5), that the excited state dipole must be small. The emission spectra in Figs. 2 and 3 display little dependence on solvent bearing out this conclusion. This is shown quantitatively in Fig. 5, where the emission data are plotted according to eqn. (5). This shows a negligible dependence of the position of the emission spectra maxima on solvent polarity for MORPIP and a weak dependence for AMINO.

Evidence for specific solvent interactions is shown in Fig. 6(a), where the Stokes' shifts for MORPIP and AMINO in diethylene glycol and glycerol do not fit the trend observed for the normal alcohols. Although diethylene glycol ($\Delta f = 0.266$) and glycerol ($\Delta f = 0.265$) have almost the same polarity as butanol ($\Delta f = 0.264$) they have larger Stokes' shifts. These solvents have two and three-dimensional hydrogen bonding networks and high viscosity, 30.2 nP for diethylene glycol and 934 nP for glycerol. Thus, because of the large difference in viscosity the solvent interaction cannot be completely modelled by Δf. However, $E_T(30)$ solvent polarity scale does provide a good fit for the Stokes' shifts for all the solutions considered here, Fig. 6(b). This is because the $E_T(30)$ scale is not model based but is an experimentally determined microscopic polarity parameter, which takes into account the solvent–solute interaction.[20]

Similarly we observe that the fluorescence quantum yields in normal alcohols are linearly dependent on Δf, but the values for diethylene glycol and glycerol do not follow this trend, as

Table 1 Stokes' shifts and quantum yields for alcohol solutions of MORPIP and AMINO at room temperature

Solvent	MORPIP		AMINO		Δf	Viscosity/nP[c]
	Stokes' shift/cm^{-1}[a]	Quantum yield (%)[b]	Stokes' shift/cm^{-1}[a]	Quantum yield (%)[b]		
Methanol	5160	0.1	7380	0.22	0.309	0.544
Ethanol	4620	0.1	6770	—	0.290	1.07
Propan-1-ol	4240	0.4	6500	0.53	0.275	1.95
Butan-1-ol	4150	0.5	6160	—	0.264	2.54
Pentan-1-ol	3970	0.7	6010	1.3	0.254	3.62
Hexan-1-ol	4010	1.0	5670	—	0.243	4.58
Diethylene glycol	5040	1.4	7990	2.32	0.266	30.2
Glycerol	5400	11.8	6630	21.8	0.265	934

[a]Accuracy ± 100 cm^{-1}. [b]Accuracy *ca.* $\pm 10\%$ of value. [c]The values of viscosity were taken from CRC solvent handbook.

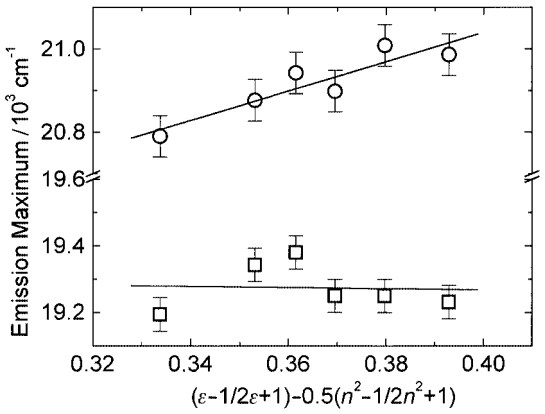

Fig. 5 Observed shifts in emission maxima, with excitation at the peak of the photo-excitation spectrum at 375 nm, for alcohol solutions of MORPIP (squares) and AMINO (circles) plotted according to eqn. (5).

shown in Fig. 7(a). The fluorescence quantum yields of the glycerol solutions are more than ten times larger than that of the normal alcohol solutions. In this instance the use of the $E_T(30)$ scale did not give a better fit to the data, Fig. 7(b). This suggests an additional effect for solutions in viscous solvents. Previous studies indicate that this is due to the constraint placed on changes in molecular conformation during excitation by the hydrogen-bonding networks.[24,25]

3.2 Glass forming solvents

Solvents that form low temperature glasses have been extensively employed as matrices for fluorophores.[45,46] If the increase in fluorescence quantum yield in viscous solvents is due to the constraining effect of the hydrogen bonding network a similar effect can be anticipated in glassy matrices. Suitable glass forming solvents are propan-1-ol,[24,47] 2MTHF[48] and EPA.[49] The use of propan-1-ol glasses allows a direct comparison to be made with the room temperature solution data. Spectra were recorded for MORPIP in propan-1-ol, 2MTHF

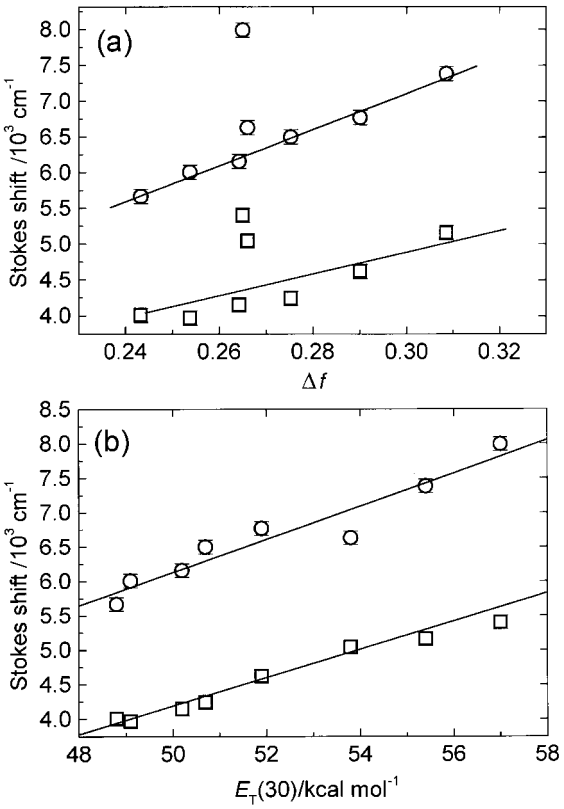

Fig. 6 Stokes' shift for alcohol solutions of MORPIP (squares) and AMINO (circles) plotted *versus* (a) Δf and (b) $E_T(30)$.

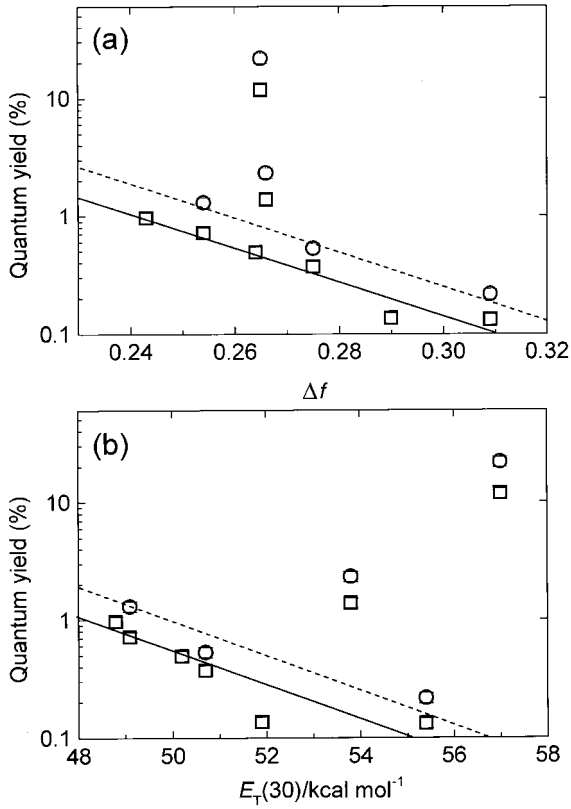

Fig. 7 Fluorescence quantum yield for alcohol solutions of MORPIP (squares) and AMINO (circles) plotted *versus* (a) Δf and (b) $E_T(30)$. The trend lines are shown for the normal alcohols; MORPIP, full line: AMINO, dashed line.

Table 2 Observed changes in spectra of MORPIP and AMINO in glass forming solvents at room and low temperature

Adduct	Solvent/K	Absorption maximum[a]/cm^{-1}	Emission maximum[b]/cm^{-1}	Absorption shift[c]/ cm^{-1} 294 to 80 K	Emission shift[d]/ cm^{-1} 294 to 80 K	Stokes' shift[e]/ cm^{-1}
MORPIP	Propanol (294)	23600	19200	1300	3000	4400
	(80)	24900	22000			2900
	2MTHF (294)	21400	18300	1300	900	3100
	(80)	22700	19200			3500
	EPA (294)	22500	19530	2600	2990	3000
	(80)	25100	22570			2600
AMINO	EPA (294)	27030	24070	1200	350	2960
	(80)	28520	24420			3830

[a]Accuracy ± 50 cm^{-1}. [b]Accuracy ± 100 cm^{-1}. [c]Accuracy ± 100 cm^{-1}. [d]Accuracy ± 100 cm^{-1}. [e]Accuracy ± 70 cm^{-1}.

and EPA glasses and for AMINO in an EPA glass. A summary of data obtained for MORPIP and AMINO at 294 K and 80 K in these solvents is given in Table 2.

The absorption and emission spectra of MORPIP in propan-1-ol as a function of temperature are shown in Fig. 8. The absorption spectra became sharper at low temperature but with no indication of any vibronic structure, the small feature just below 26000 cm^{-1} is an instrumental artefact. Thus, inhomogeneous broadening[50] dominates even at 80 K. There is an increase in optical density, which is commensurate with the observed narrowing of the absorption band and increase in sample density. Both the absorption and fluorescence maxima shift to higher energy as the solvent density, ε, n and the polarity parameter (Δf) increase at low temperatures as expected for $\mu_e < \mu_g$, *cf.* eqns. (4) and (5). However, the emission maximum shifts by a larger amount than the absorption maximum on cooling, *cf.* Fig. 8. This is the opposite of what is expected for $\mu_e < \mu_g$. The nett effect is that the Stokes' shift decreases from *ca.* 4400 cm^{-1} at room temperature to *ca.* 2900 cm^{-1} at 80 K rather than increasing as indicated by eqn. (3). Thus, the constraint placed on molecular conformation by the glassy matrix has a significant effect on the emission process. Precise determinations were not made of the fluorescence quantum efficiencies below room temperature. However, a dramatic increase in emission intensity was observed in the glassy phase, which is formed at *ca.* 200 K, *cf.* Fig. 8(b). The integrated emission intensity rises sharply below 250K becoming approximately constant below 200 K, Fig. 10. The quantum yield is estimated to be 13% at 80 K compared with room temperature value of 0.4%. Non-radiative decay is reduced at low temperature as thermally activated processes are turned off.[44] The increase of emission intensities is influenced both by this and by changes in the interaction of the MORPIP with the host medium.

In contrast the data for MORPIP in 2MTHF, Table 2, show that the maximum of the absorption and emission spectra shifts by smaller, similar, amounts between 294 K and 80 K. Consequently, there is a small increase in Stokes' shift between 294 K and 80 K. If this shift is attributed solely to the solvatochromic shift, which results from the density change of the medium, then on the basis of the trend line in Fig. 4(b) Δf must increase by *ca.* 0.02 between 294 K and 80 K. While data are available for the relative permittivity (ε) over the range 296 K to 208 K comparable data are not available for the refractive index (n); however, on the basis of data for similar solvents Δf should increase by *ca.* 0.03 over this temperature range. Thus, the observed change in Stokes' shift is somewhat smaller than expected if it is due solely to solvatochromism. Emission spectra of MORPIP in 2MTHF at various temperatures are shown in Fig. 9. The increase in emission intensity (*i.e.* quantum yield) at low temperatures is similar to that for the propan-1-ol glass, *cf.* Fig. 10.

For MORPIP in EPA the shifts in the maximum in absorption and emission between 294 and 80 K are similar and there is a small decrease in the Stokes' shift, *cf.* Table 2. Over the same temperature range there is a distinct difference between the shifts with temperature for the maximum in absorption and emission of AMINO in EPA although the values are the smallest measured, *cf.* Table 2. This results in a significant increase in Stokes' shift for AMINO in comparison to a decrease for MORPIP.

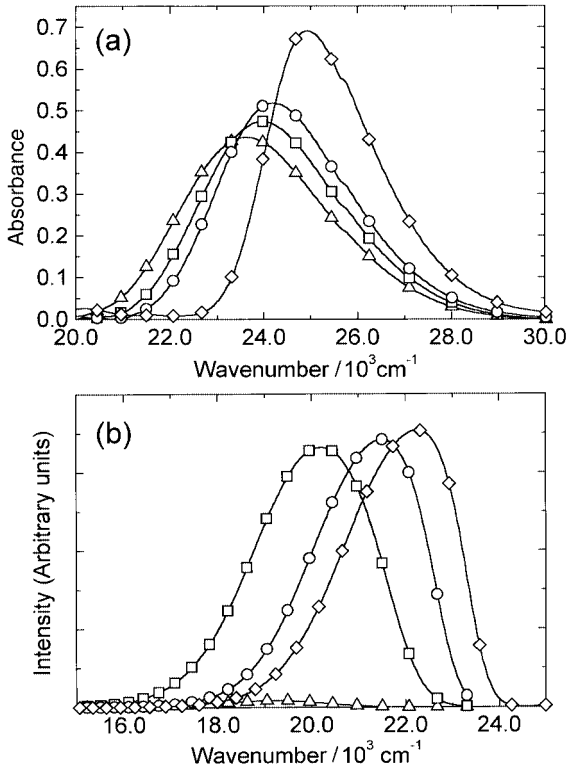

Fig. 8 (a) Absorption and (b) emission spectra of MORPIP in propan-1-ol at 294 (triangles), 200 (squares), 150 (circles) and 80 K (diamonds).

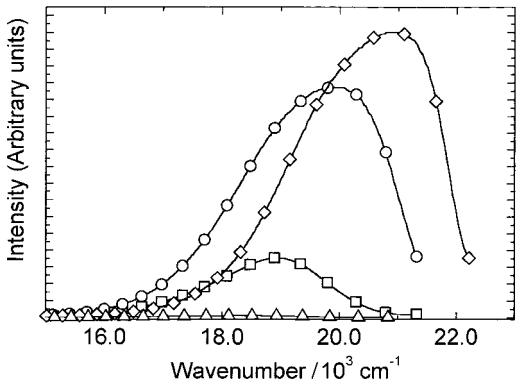

Fig. 9 Emission spectra of MORPIP in 2-methyl THF at 294 (triangles), 200 (squares), 150 (circles) and 80 K (diamonds).

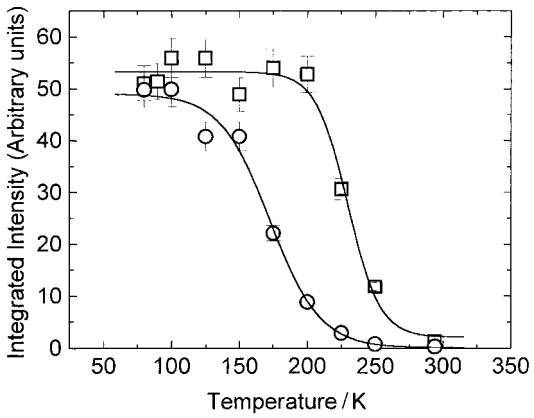

Fig. 10 Integrated emission intensity of MORPIP in propan-1-ol (squares) and 2-methyl THF (circles) as a function of temperature.

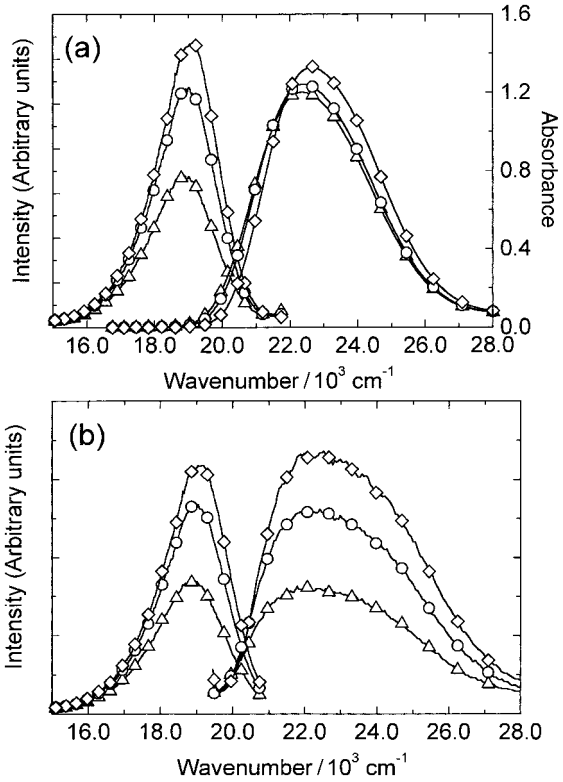

Fig. 11 Spectra of the MORPIP doped PMMA films (a) absorption (right) and emission (left) for films cast from DMF solution at 294 (triangles), 200 (circles) and 80K (diamonds), (b) excitation (right) and emission (left) for films cast from TMU solution at 294 (triangles), 200 (circles) and 80 K (diamonds).

3.3 Crystalline powders

Fluorescence from a TCNQ adduct was first observed visually for microcrystalline powder of MORPIP formed above an acetonitrile solution in a test tube. The fluorescence quantum yields were determined for thin layers of MORPIP and AMINO micro-crystals spread on a non-fluorescent silica substrate in the integrating sphere apparatus. Values of 5% and 1.6% were obtained for the photoluminescence quantum yields of MORPIP and AMINO, respectively. These values are approximate since there was considerable variation between samples, which we attribute to variations in the size of microcrystallites from sample to sample.

3.4 Polymer matrices

Films of PMMA and PC containing MORPIP and AMINO were prepared by spin and dip coating. PMMA films containing MORPIP were obtained from solutions in DMF, tetramethylurea (TMU) and dichloromethane and films containing AMINO were obtained from DMF and TMU solutions. PC films containing MORPIP were obtained from DCM solutions. These films were used to determine fluorescence quantum yields at room temperature, in the integrating sphere apparatus, and study the temperature dependence of the absorption and emission spectra from room temperature down to 80 K. Absorption and emission spectra for films containing MORPIP prepared from DMF and TMU solutions at room temperature, 200 and 80 K are shown in Fig. 11. Room temperature and low temperature data are listed in Tables 3 and 4, respectively. Quantitative data were not obtained for the AMINO samples but qualitatively the emission observed was comparable to that from the MORPIP in PC sample.

At 80 K the intensities of emission for MORPIP in the PMMA films prepared from TMU and DMF solutions was about 2 and 3 larger than that at 294 K, *cf.* Fig. 11. This is in contrast with the much larger increase, *ca.* thirty to one hundred times, of the emission intensity between room and low temperature in glass forming solvents. PMMA is below its glass transition temperature at room temperature and the increase in density on cooling will be *ca.* 1–2%. This is much smaller than that of the glass forming solvents, *e.g.* EPA contracts by *ca.* 25% between room and liquid nitrogen temperatures.

3.5 Fluorescence decay times

The fluorescence lifetime of MORPIP in propan-1-ol was determined at 294 and 80 K by the time resolved single photon counting technique. The sample was excited at 340 nm and the

Table 4 Low temperature absorption and emission data for polymer films containing MORPIP obtained from DMF and TMU solutions

Casting solvent	Temperature/ K	Absorption maximum[a]/ cm^{-1}	Emission maximum[a]/ cm^{-1}	Stokes' shift[b]/ cm^{-1}
DMF	294	22400	18200	4200
	200	22400	18500	3900
	80	22700	18700	4000
TMU	294	22400	18900	3500
	200	22400	1900	3400
	80	22600	19200	3500

[a]Accuracy ± 100 cm^{-1}. [b]Accuracy ± 200 cm^{-1}.

Table 3 Room temperature absorption and emission data for polymer films containing MORPIP and AMINO obtained from different solvents

Adduct	Polymer	Casting solvent	Absorption maximum[a]/cm^{-1}	Emission maximum[a]/cm^{-1}	Stokes' shift[b]/cm^{-1}	Quantum yield (%)[c]
MORPIP	PMMA	DMF	22620	19100	3520	21
		TMU	22570	19250	3320	21
		DCM	22420	18760	3660	19
	PC	DCM	21930	18330	3600	7 ± 2
AMINO	PMMA	DMF	26950	21210	5740	[d]
		TMU	26980	21340	5640	[d]

[a]Accuracy ± 50 cm^{-1}. [b]Accuracy ± 100 cm^{-1}. [c]Accurate to ± 5% of value unless noted. [d]See text.

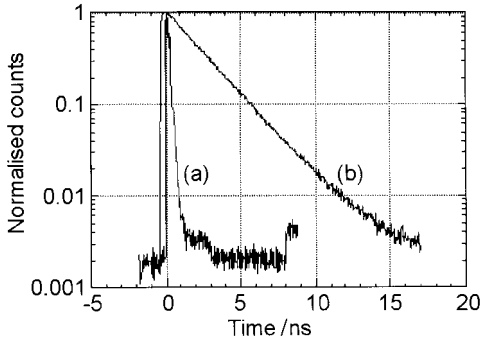

Fig. 12 Fluorescence decay of the emission of MORPIP dissolved in propan-1-ol at (a) 294 and (b) 80 K.

emission was detected at 520 nm at 294K and 450 nm at 80 K close to the emission maximum at these temperatures, *cf.* Table 2. The fluorescence decays observed are shown in Fig. 12. The decay time at room temperature was too short to measure the temporal profile of the observed emission being essentially identical with that of the excitation pulse. Thus the decay time must be less than *ca.* 0.1 of the width of the excitation pulse, *i.e.* <10 ps. The fluorescence decay from a sample at 80 K was fitted with a single exponential decay with a lifetime of 2.5 ± 0.2 nanoseconds, *cf.* the linearity of the decay over two decades shown in Fig. 12. The quality of fit was good with a raw reduced chi-squared of 1.1 and random weighted residuals.[29]

4. Discussion

In principle eqns. (3) to (5) can be used to estimate the μ_g and μ_e for MORPIP and AMINO. However, the values obtained depend crucially on the factor a^3, where a is the radius of the Onsager cavity enclosing the molecule in solution. The model of a spherical cavity is widely applied although it is clear that for elongated molecules a more complex model with an ellipsoidal cavity should be used.[10,51] While this approach is strictly correct the additional complication is not justified given the approximations involved in the analysis. Furthermore it has been shown that the equivalent radius of the spherical cavity deduced from crystal structure data is in reasonable agreement with that found experimentally for other zwitterionic molecules.[10] The crystal structure of MORPIP gives a volume per molecule of *ca.* 530 Å^3.[11,13] If this is taken as the volume of the Onsager cavity then $a\approx4$ Å, which represents a lower bound for the solution cavity.[10] The slopes of the plots of absorption and emission maxima and the Stokes shift for MORPIP, Figs. 4 and 5, are 19700 ± 3300 cm^{-1} ($R=0.948$), 160 ± 1700 cm^{-1} ($R=-0.049$) and 18100 ± 2800 cm^{-1} ($R=0.956$), respectively. Using these data the values found from eqns. (3) to (5) are $\mu_g=12\pm5$ D and $\mu_e=-0.1\pm1$ D. Modifying eqns. (4) and (5) to allow for $\mu_e\ll\mu_g$, *i.e.* replacing $\mu_g(\mu_e-\mu_g)$ by μ_g^2 in eqn. (4) and $\mu_e(\mu_e-\mu_g)$ by $\mu_e\,\mu_g$ in eqn. (5), has little effect on these values giving $\mu_g=11\pm5$ D and $\mu_e=-0.1\pm1$ D. The value obtained for μ_g from the spectral data is similar to that of 15 D found both theoretically and experimentally, in chloroform, dichloromethane and acetone, for MORPIP.[11,13] This agreement is reasonable given the approximations involved in the theory and the choice of a, the ellipsoidal shape of the molecules and the large value of μ_g.

Crystal structure data are not available for AMINO. However, although AMINO has only one bulky substituent the molecular volume will be similar to that of MORPIP so that $a\approx4$ Å is a reasonable approximation. The slopes of the plots of absorption and emission maxima and the Stokes shift for AMINO, Figs. 4 and 5, are 32400 ± 2700 cm^{-1} ($R=0.984$), 3500 ± 800 cm^{-1} ($R=0.913$) and 25100 ± 1200 cm^{-1} ($R=0.995$), respectively. In this case from eqns. (3) to (5) we find that $\mu_g=16\pm3$ D and $\mu_e=2\pm1$ D or using the approximation $\mu_e\ll\mu_g$ the values are again unchanged within the experimental error, $\mu_g=14\pm3$ D and $\mu_e=1.5\pm1$ D.

The alternative fitting procedure due to Koutek[52] has been shown by Ravi *et al.*[53] and Kumar *et al.*[54] to give reasonable results for μ_e for molecules with modest μ_g, *i.e.* 3–7 D. However, the agreement with the limited experimental data is not good in this case. Fitting data for MORPIP and AMINO leads to values for both molecules for μ_g and μ_e of *ca.* 5 and 1 D, respectively. The former is much smaller than the value of 15 D determined experimentally for MORPIP and the latter does not reflect the difference in solvent dependence of the fluorescence between AMINO and MORPIP, Fig. 5.

The fluorescence quantum yields of MORPIP and AMINO dissolved in normal alcohols fall in the range 0.1 to 1% (Table 1). The presence of oxygen has little effect, as the excited state lifetime is too short to allow for diffusion to permit interaction with the dissolved oxygen. The quantum yields are larger, up to 20%, in the viscous solvents diethylene glycol and glycerol. The values for AMINO are about twice those found for MORPIP in the same solvent. When the Stokes' shifts are plotted as a function of polarity parameter (Δf) the results for the viscous solvents depart from the trend for the other alcohols, Fig. 6(a). Although this discrepancy is removed when the parameter $E_T(30)$ is used rather than Δf, Fig. 6(b), the quantum yield data for the viscous solvents remain anomalous, Fig. 7, showing a strong effect of solvent viscosity on fluorescence intensity. The fluorescence properties of chromophores, which undergo large conformational changes on photoexcitation, are strongly influenced by solvent viscosity. Tetraphenylethylene (TPE) has been extensively studied.[25,55,56] The lifetime of TPE increases from 6 ps in low viscosity solvents to 60 ps in ethylene glycol and 600 ps in glycerol.[25] This has been attributed to the viscous media hindering the rotation of the phenylene moieties thereby limiting non-radiative decay of the excited state, which is induced by the torsion motion of the phenylenes. A decrease in non-radiative decay will lead to an increase in fluorescence quantum yield as observed for MORPIP and AMINO.

There is other experimental evidence that there are significant conformational changes between ground and excited state in the TCNQ adducts. As noted earlier X-ray crystallographic data show that the electron donor moieties (amino groups) and the π-conjugation unit (the benzene ring) in the TCNQ adducts are not coplanar.[6,9,26,30] In MORPIP and related compounds the twist angle between the molecular components in the molecular ground state is approximately 45°. Despite this, both theory and experiment show that the ground state dipole moments of these molecules are large.[6,10,11,13,32] As noted above for MORPIP μ_g is found to be approximately constant at 15 D in chloroform, dichoromethane and acetone solutions. This is in accord with the result that for alcohol solutions the change in dipole moment on excitation is constant and $\mu_e\cong0$, *i.e.* μ_g is approximately constant. This behaviour is somewhat different from that of adducts made with tertiary amines, which are rigid planar molecules. The dipole moments of these molecules increase as the polarity of the solvent is increased.[10,57] Thus, we deduce that the molecular geometry of MORPIP does not remain fixed as the molecular environment, *e.g.* solvent polarity, is changed. The small value of μ_e is, therefore, likely to be a consequence of a change in the torsion angle between the component parts of the molecule in the excited state.

MOPAC96-AMI calculations give a larger value for μ_e for a planar geometry (~10 D) than for a 90° twist (~6 D).[7] However, these values are significantly larger than we find experimentally. Recently similar calculations have been performed for a series of adducts with twist angles between ~40° to ~75° and give values for μ_e in the range 9 to 13 D.[32] These values are all much larger than our results for μ_e. However,

theoretical modelling using *ab initio* methods shows that the dipole moment increases as the twist angle increases and that the excited state has a more planar geometry. Hence, we believe that in low viscosity solvents these molecules undergo significant changes in conformation on photo-excitation. Restriction of the change in molecular conformation by viscous solvents leads to enhanced fluorescence; *i.e.* the relaxed excited state has a low fluorescence quantum yield, while that of the hindered excited state is much higher.

We note that the steric hindrance for AMINO, due to the bulky cyclohexyl group attached to the cyclic substituent will be much greater than for MORPIP, see Fig. 1. Molecular modelling shows that a twist angle of 45° between the molecular sub-units is possible for AMINO, with some slight deformation of the molecular framework. However, a large reduction in twist angle on excitation is not possible. This suggests a smaller change in molecular conformation for AMINO than for MORPIP both as a function of solvent polarity and on excitation. It also offers an explanation for the non-zero value of μ_e for AMINO and the higher fluorescence intensity for AMINO in all the solvents used. As the viscosity of diethylene glycol and glycerol is derived from a hydrogen-bonding network they will interact strongly with AMINO and produce significant effects on the fluorescence despite the lower flexibility of this molecule.

This hypothesis is also capable of explaining the trends observed with solid matrices. The molecular packing in a crystal lattice will leave limited free volume for molecular deformation on photo-excitation. Hence, larger fluorescence quantum efficiency is to be expected for crystals than for solutions with a larger effect for the more flexible MORPIP, as observed.

The same considerations apply to polymer matrices and glass forming solvents. The differences in spectra and fluorescence quantum yield in the polymer matrices reflect both the polarity and density of the media. PC has a higher polarity than PMMA and a distinct spectral shift is observed. The differences in quantum efficiency reflect differences in the free volume available in the different polymers. Although fluorescence intensity for MORPIP in glass forming solvents was not determined as precisely as that of the room temperature solutions and films a dramatic increase from an initially small value was observed on cooling to 80 K. This reflects the change from a fluid to a solid environment as the glass forms. Initially the adduct is free to relax with minimal constraint giving a low fluorescence quantum efficiency. This increases as the solvent viscosity increases constraining the changes in molecular conformation on excitation and becomes constant as the glass solidifies into a phase with low thermal expansion, *cf.* Fig. 10. The increase in fluorescence for polymer films over the same temperature range was much smaller. This is to be expected as the polymer matrix is in a glassy phase throughout this temperature range and the reduction in free volume on cooling is small. It is surprising that the fluorescence quantum yields for the polymer films are approximately four times the values observed for crystals. A possible explanation is that the environment in a crystal is identical for all molecules while in the polymer film there is a distribution of environments due to variation in the size of the cavities, which provide the free volume, at the molecular level. Thus the higher fluorescence intensity observed in the polymer films will predominantly originate from molecules in the most constrained environments.

The fluorescence lifetime measurements provide further evidence that rapid non-radiative decay occurs when the adducts are dissolved in low viscosity solvents while viscous and solid matrices constrain molecular relaxation and open up a radiative decay channel. The decay of the fluorescence of MORPIP in propanol at room temperature, shown in Fig. 12(a), is identical with the laser excitation pulse. Thus, the excited molecules decay on a time scale either comparable to or shorter than the instrumental resolution, *i.e.* $\leqslant$10 ps. However, at 80 K in the glassy matrix the decay is well characterised by a single exponential with a time constant of 2.5 ns, Fig. 12(b). Some increase in fluorescence and lifetime is to be expected at low temperatures due to the reduction in thermally induced non-radiative decay. However, the large changes observed are indicative of a significant change in the character of the emission process, from a predominantly non-radiative process in solution at room temperature to a predominantly radiative process in the glass at low temperature.

Similar data have been obtained for other adducts with different substituents so we believe that the behaviour reported here for MORPIP and AMINO is representative of this class of compounds. The molecules have large μ_g and a molecular conformation in which the plane of the substituents is twisted with respect to the conjugated ring and CN moieties. When the molecules are free to relax on excitation μ_e is small and the molecular geometry of the excited state is less twisted than that of the ground state and may in some instances be close to planar, *e.g.* MORPIP. At room temperature the decay from this state is predominantly non-radiative. In situations where the molecular relaxation is inhibited by constraints imposed by the environment, decay by a radiative process is favoured. This behaviour may be viewed as an inverse of that where the ground state is planar and the excited state is twisted with greater charge transfer in the excited state, *i.e.* TICT (twisted intramolecular charge transfer).[34–37,39]

Acknowledgements

This work was supported by grants from the Engineering and Science Research Council (EPSRC). We thank Dr I. D. W. Samuel and M. Halim for making preliminary measurements of the fluorescence of the solid samples at room temperature and N.-A. Hackman for assistance in preparation of polymer film samples.

References

1 D. S. Acker, R. J. Harder, W. R. Hertler, W. Mahler, L. R. Melby, R. E. Benson and W. E. Mochel, *J. Am. Chem. Soc.*, 1960, **82**, 6408.
2 D. S. Acker and W. R. Hertler, *J. Am. Chem. Soc.*, 1962, **84**, 3370 and following papers (Substituted Quinodimethanes Parts I to V).
3 B. P. Bespalov and V. V. Titov, *Russ. Chem. Rev.*, 1975, **44**, 1091.
4 G. J. Ashwell, E. J. C. Dawnay, A. P. Kuczyñski, M. Szablewski, I. M. Sandy, M. R. Bryce, A. M. Grainger and M. Hasan, *J. Chem. Soc., Faraday Trans.*, 1990, **86**, 1117.
5 N. Martin, J. L. Segura and C. Seoane, *J. Mater. Chem.*, 1997, **7**, 1661.
6 M. Ravi, S. Cohen, I. Agranay and T. P. Radhakrishnan, *Struct. Chem.*, 1996, **7**, 225.
7 M. Ravi, D. N. Rao, S. Cohen, I. Agranat and T. P. Radhakirishnan, *Chem. Mater.*, 1997, **9**, 830.
8 M. Ravi, *Proc. Indian Acad. Sci. (Chem. Sci.)*, 1998, **110**, 133.
9 M. Ravi, P. Gangopadhyay, D. N. Rao, S. Cohen, I. Agranat and T. P. Radhakrishnan, *Chem. Mater.*, 1998, **10**, 2371.
10 M. Szablewski, P. R. Thomas, A. Thornton, D. Bloor, G. H. Cross, J. M. Cole, J. A. K. Howard, M. Malagoli, F. Meyers, J. Brédas, W. Wenseleers and E. Goovaerts, *J. Am. Chem. Soc.*, 1997, **119**, 3144.
11 Y. Kagawa, Ph.D. Thesis, University of Durham, 1998.
12 S. R. Marder and J. W. Perry, *Science*, 1994, **263**, 1706.
13 Y. Kagawa, M. Szablewski, M. Ravi, N.-A. Hackman, G. H. Cross, D. Bloor, A. S. Batsanov and J. A. K. Howard, *Nonlinear Opt.*, 1999, **22**, 235.
14 J. H. Burroughes, D. C. Bradley, A. R. Brown, R. N. Marks, K. M. Makay, R. H. Friend, P. L. Burns and A. B. Holmes, *Nature*, 1990, **347**, 539.
15 D. Braun and A. J. Heeger, *Appl. Phys. Lett.*, 1991, **58**, 1982.
16 H. Tanaka, S. Tokito, Y. Taga and A. Okada, *J. Mater. Chem.*, 1998, **8**, 1999.
17 F. Hide, M. A. Diaz-Garcia, B. J. Schwartz, M. R. Andersson, Q. Pei and A. J. Heeger, *Science*, 1996, **273**, 1833.

18 N. Tessler, P. K. H. Ho, V. Cleave, D. J. Pinner, R. H. Friend, G. Yahioglu, P. L. Barny, J. Gray, M. de Souza and G. Rumbles, *Thin Solid Films*, 1999, **363**, 64.
19 J. R. Lakowicz, *Principles of Fluorescence Spectroscopy*, 2nd Edn., Kluwer Academic/Plenum Publishers, New York, 1999.
20 C. Reichart, *Chem. Rev.*, 1994, **94**, 2319.
21 A. D. Osborne, *J. Chem. Soc., Faraday Trans. 2*, 1980, **76**, 1638.
22 K. G. Casey and E. L. Quitevis, *J. Phys. Chem.*, 1988, **92**, 6590.
23 K. M. Keery and G. R. Fleming, *Chem. Phys. Lett.*, 1982, **93**, 322.
24 C. J. Tredwell and A. D. Osborne, *J. Chem. Soc., Faraday Trans. 2*, 1980, **76**, 1627.
25 P. F. Barbara, S. D. Rand and P. M. Rentzepis, *J. Am. Chem. Soc.*, 1981, **103**, 2156.
26 Y. Kagawa, M. Szablewski, M. Ravi, N.-A. Hackman, G. H. Cross, D. Bloor, A. S. Batsanov and J. A. K. Howard, in preparation.
27 W. H. Melhuish, *J. Phys. Chem.*, 1961, **65**, 229.
28 J. C. de Mello, H. F. Wittmann and R. H. Friend, *Adv. Mater.*, 1997, **9**, 230.
29 D. J. R. Birch and R. E. Imhof, in *Topics in Fluorescence Spectroscopy*, ed. J. R. Lakowicz, Volume 1, Techniques, Plenum Press, New York, 1991, pp. 1–95.
30 J. C. Cole, J. M. Cole, G. H. Cross, M. Farsari, J. A. K. Howard and M. Szablewski, *Acta Crystallogr.*, 1997, **B53**, 812.
31 J. Onsager, *J. Am. Chem. Soc.*, 1936, **58**, 1486.
32 P. Gangopadhay, M. Ravi and T. P. Radhakrishnan, *Indian J. Chem.*, 2000, **39A**, 106.
33 D. Grasso and E. Bellio, *Chem. Phys. Lett.*, 1975, **30**, 421.
34 H. Lami and N. Glasser, *J. Chem. Phys.*, 1986, **84**, 597.
35 J-F. Létard, R. Lapouyade and W. Rettig, *J. Am. Chem. Soc.*, 1993, **115**, 2441.
36 G. Liu, L. Heisler, L. Li and M. G. Steinmetz, *J. Am. Chem. Soc.*, 1996, **118**, 11412.
37 C. F. Zhao, R. Gvishi, U. Narang, G. Ruland and P. N. Prasad, *J. Phys. Chem.*, 1996, **100**, 4526.
38 J. Herbich and A. Kapturkiewicz, *J. Am. Chem. Soc.*, 1998, **120**, 1014.
39 K. Araki, K. Tada, M. Abe and T. Mutai, *J. Chem. Soc., Perkin Trans. 2*, 1998, 1391.
40 A. T. Amos and B. L. Burrows, *Adv. Quant. Chem.*, 1973, **7**, 289.
41 C. Streck and R. Reichert, *Ber. Bunsen-Ges. Phys. Chem.*, 1994, **98**, 619.
42 B. Cunderlíková and L. Šikurová, *Chem. Phys.*, 2001, **263**, 415.
43 P. Suppan, *J. Photochem. Photobiol. A. Chem.*, 1990, **50**, 293.
44 M. Fall, J.-J. Aaron, M. M. Dieng and C. Párkányi, *Polymer*, 2000, **41**, 4047.
45 P. F. Barbara, P. M. Rentzpis and L. E. Brus, *J. Am. Chem. Soc.*, 1980, **102**, 2786.
46 H. T. Oh, Y. Kanematsu, A. Kurita and T. Kushida, *J. Luminescence*, 1996, **66/67**, 310.
47 E. Laitinen, K. Salonen and T. Harju, *J. Chem. Phys.*, 1996, **105**, 9771.
48 R. Reichart, F. Stickel, R. S. Fee and M. Maroncelli, *Chem. Phys. Lett.*, 1994, **229**, 302.
49 S. L. Murov, I. Charmichael and G. L. Hug, *The Handbook of Photochemistry*, Marcel Dekker, London, 1993.
50 N. A. Nemkovich, A. N. Rubinov and V. I. Tomin, *Topics in Fluorescence Spectroscopy*, ed. J. R. Lakowicz, Volume 2. Principles, Plenum Press, New York, 1991, pp. 367–428.
51 C. J. F. Böttcher, *Theory of Electric Polarization*, Elsevier, Amsterdam, 1973, Vol. 1; 1978, Vol. 2.
52 B. Koutek, *Collect. Czech. Chem. Commun.*, 1978, **43**, 2368.
53 M. Ravi, A. Samanta and T. P. Radhakrishnan, *J. Chem. Phys.*, 1994, **98**, 9133.
54 S. Kumar, V. C. Rao and R. S. Rastogi, *Spectrochim. Acta, Part A*, 2001, **57**, 41.
55 J. Kordas and M. A. El-Bayoumi, *J. Am. Chem. Soc.*, 1974, **96**, 3043.
56 D. Ben-Amotz and C. B. Harris, *Chem. Phys. Lett.*, 1985, **119**, 305.
57 P. R. Thomas, Ph.D. Thesis, University of Durham, 1997.